sen for the ability of the electrode to detect a substrate or product, and the procedure can be modified in order to be adapted to the chosen electrode. The procedures described in this paper offer several advantages: a) The immobilization of the enzyme by glutaradehyde gives chemical bonds which result in a good stabilization of the enzyme molecules, more efficient than entrapment techniques when fragile enzymes are concerned. b) No leaching or unhomogeneous distribution results, no matter what the size of the enzyme molecules. Thus, there is no need of adding an extra barrier (such as cellophane) between the active layer and the unknown sample. c) Such homogeneous and stable layers are ideally suited for systematical analysis of the parameters controlling the enzyme electrode response.

It was shown that the cosubstrate (O_2) or product concentration on the surface of the electrode is a simple function of the unknown substrate concentration in the solution when this concentration is lower than K_m. Under these conditions the system can act as a sensor.

The ease of the achievement of such layers and membranes, and the versatility of the procedure can be specially useful in such cases as: a) Quick construction of an electrode adapted to a special need (time of preparation often shorter than 15 minutes). b) Construction of sequential multienzyme electrodes. c) Application to biological fluids: the possibility of using selective gas electrodes allows measurements in complex media such as human plasma or urine. As long as the electrode is used in a not septic medium, such as blood plasma or fresh urine, no protection of the active elect ode is necessary. For a very septic medium, a cellophane protection may be necessary from bacterial contamination.

Miniaturization of such versatile electrodes may allow their use in vivo in the future by taking advantage of the proteic coating of the permselective hydrophobic membrane, and of the pseudo steady-state equilibrium between inward diffusing substrate and outward diffusing product for every concentration of substrate in the medium. With this end in view, it was necessary to study the range of concentration, the parameters, and the possibilities of their use. The confrontation of theoretical analysis with experimental measurements helps in their analysis and outlines their utility in a variety of biological media.

ACKNOWLEDGMENT

The authors are indebted to Pr. Kernevez for numerical analysis on the computer.

LITERATURE CITED

(1) G. P. Hicks and S. K. Updike, *Anal Chem.*, **38,** 726 (1966).
(2) S. J. Updike and G. P. Hicks, *Nature (London)*, **214,** 936 (1967).
(3) S. J. Updike and G. P. Hicks, *Science*, **270,** 158 (1967).
(4) G. G. Guilbault and J. G. Montalvo, *J. Am. Chem Soc.*, **92,** 2533 (1970).
(5) G. G. Guilbault and J. G. Montalvo *J. Anal. Lett.*, **2** (5), 283 (1969).
(6) G. G. Guilbault, R. K. Smith, and J. G. Montalvo, *Anal. Chem.*, **41,** 600 (1969).
(7) G. G. Guilbault and E. Hrabankova, *Anal. Chem.*, **42,** 1779 (1970).
(8) G. G. Guilbault, *Biotechnol. Bioeng. Symp.*, **3,** 361 (1972).
(9) G. G. Guilbault and J. Das, *Anal. Biochem.*, **33,** 341 (1970).
(10) T. Anfalt, A. Graneli and D. Wagner, *Anal. Lett.* **6,** 969 (1973).
(11) C. Tran-Minh, E. Selegny, and G. Broun, *C. R. Acad. Sci. Paris*, **275** (C), 309 (1972).
(12) G. G. Guilbault and F. Shu, *Anal. Chem.*, **44,** 2161 (1972).
(13) C. Tran-Minh and G. Broun, *C. R. Acad Sci. Paris*, **276** (D), 2215 (1973).
(14) D. Thomas, G. Broun, and E. Selegny, *Biochimie*, **54,** 229 (1972).
(15) J. P. Kernevez, Thesis, Paris (1972).
(16) E. Selegny, J. P. Kernevez, G. Broun, and D. Thomas, *Physiol. Veg.*, **9** (1) 51 (1971).
(17) C. Tran-Minh, Thesis, 1971, Rouen (France) AO 6262 - C.N.R.S.
(18) G. Broun, E. Selegny, C. Tran-Minh, and D. Thomas, *FEBS Lett.*, **7,** 223 (1970).
(19) L. A. Greddes and L. E. Baker, "Principles of Applied Biomedical Instrumentation", John Wiley and Sons, New York, 1968.
(20) H. Kaiser *Pure Appl. Chem.*, **34,** 35 (1973).
(21) G. Broun, C. Tran-Minh, D. Thomas, D. Domurado, and E. Selegny, *Trans. Am. Soc. Artif. Int. Org.*, **17,** 341 (1971).
(22) A. M. Berjonneau, C. Tran-Minh, and G. Broun, *C. R. Acad. Sci. Paris*, **275** (D), 121 (1972).
(23) A. M. Berjonneau, C. Tran-Minh, and D. Thomas, Symposium sur les protéines chimiquement geffées et réticulées, Rouen, 1972.

RECEIVED for review October 12, 1973. Accepted January 28, 1975. This work was done under contract 72.7.0073 with Delegation Générale à la Recherche Scientifique et Technique (D.G.R.S.T.)

Mercury Film Nickel Minigrid Optically Transparent Thin Layer Electrochemical Cell

William R. Heineman,[1] Thomas P. DeAngelis, and John F. Goelz

Department of Chemistry, University of Cincinnati, Cincinnati, OH 45221

An optically transparent thin layer electrochemical cell with characteristics of a mercury electrode has been prepared by electrochemically depositing a thin film of mercury onto a 333 lpi, 57% transmittant nickel minigrid. The mercury film of ~200-Å thickness caused the hydrogen overvoltage to shift 500–600 mV negative of its value on nickel. This shift enabled spectroelectrochemical measurements to be made on reduction processes that were obscured by hydrogen evolution on other electrode materials used in transparent thin layer cells. This was demonstrated with spectroelectrochemical measurements on the reduction of methyl viologen dication. The thin layer electrode proved adaptable to analysis of metal ions by differential pulse anodic stripping voltammetry and anodic stripping coulometry. The sensitivity of differential pulse anodic stripping voltammetry combined with the small volume capabilities (50 μl) of the thin layer cell make the mercury film thin layer electrode useful for trace analysis of metal ions in very small amounts of solution.

The use of optical techniques in conjunction with electrochemical measurements has proved increasingly useful in the study of electrode processes (*1–3*). One such spectroelectrochemical method which combines the rapid exhaustive electrolysis of thin layer cells with the simplicity

[1] Author to whom correspondence should be addressed.

of transmission spectroscopy is the optically transparent thin layer electrode (*4, 5*). This method has been used mainly for recording spectra of various redox states in the systems studied (*6–11*). A recent application uses the cell for precision measurement of enzyme E°′ values by a spectropotentiostatic technique (*12*).

The electrode materials for transparent thin layer cells have been limited to gold minigrids (*4*) and vapor-deposited platinum films (*5, 11*). The desirability for expanding this electrode selection to include a mercury optically transparent electrode is derived from two characteristics of mercury. Its greater hydrogen overvoltage extends the negative potential limit, and the electrochemistry of metal ions being reduced to their metallic state is generally more well-behaved on mercury than on solid electrodes (*13*). Also, since a substantial proportion of electrochemical measurements are made on mercury, the ability to obtain spectroelectrochemical information on mercury for a particular chemical system can be useful.

This report describes a mercury film transparent electrode which was prepared by electrochemical deposition of mercury on a nickel minigrid. Good optical transparency was obtained by using the nickel minigrid as a solid framework for the liquid mercury. Electrochemical characteristics of the electrode and its utility for optical and analytical applications were investigated using the electrode in the thin-layer cell configuration of the minigrid-microscope slide variety (*4, 12*).

EXPERIMENTAL

Apparatus. Optically transparent thin layer electrochemical cells were assembled from microscope slides, Teflon tape spacers, and minigrid electrodes as reported previously (*4, 12*). The transparent electrodes were 333 lines per inch, 57% transmittant nickel minigrids (Buckbee Mears Co., St. Paul, MN). The dimensions of the minigrid within the thin layer cell were approximately 1 cm × 1.8 cm. Two layers of 2-mil pressure sensitive Fluorofilm DF-1200 Teflon tape (Dilectrix Corp., Farmingdale, NY) were used as spacers. This gave approximate cell thickness of 0.015 to 0.020 cm and cell volumes of 30–35 μl. Electrodes were kept in a 110 °C oven for 12 hours after assembly to cure the epoxy which held the cells together.

A Lucite frame was used to position the thin layer cell and the reference and auxiliary electrodes in the 5-ml cup which contained the solution to be studied.

All potential measurements were vs. a saturated calomel electrode.

The potentiostat used for electrochemical measurements was of conventional operational amplifier design. System response signals were recorded on a Houston Instrument 2200-5-6 x-y recorder with time base.

A Princeton Applied Research Model 174 polarographic analyzer was used for the differential pulse polarography measurements in the thin layer cell and for cyclic voltammograms on a hanging mercury drop electrode.

Optical experiments were performed in a spectrophotometer consisting of a tungsten lamp source, a Schoeffel GM 100 miniature grating monochromator, and a PIN-10 DP planar diffused silicon photodiode (United Detector Technology, Inc.) connected to an operational amplifier current to voltage converter. Voltage output was monitored with a Fluke 8000A Digital Multimeter.

Micrographs were taken with a JEOL JSM-U3 scanning electron microscope. To retard evaporation of mercury in the vacuum, the mercury-coated minigrids were mounted on a cold stage cooled to −45° by Freon 502.

Reagents. The mercuric solution used for depositing mercury on nickel was 0.20–1.00m*M* $Hg(NO_3)_2 \cdot H_2O$ (Baker, Analyzed) in either of three aqueous solutions: (1) 0.1*M* HCl, 0.5*M* KCl; (2) 0.2*M* sodium acetate adjusted to pH 4.0 with HCl, 0.5*M* KCl; or (3) 0.1*M* phosphate buffer, pH 7.00 (Buffer-Titrisol, EM Laboratories, Elmsford, NY), 0.5*M* KCl. Methyl viologen dichloride (K & K Laboratories) was used without further purification. Lead, cadmium, and thallium solutions were prepared from $Pb(NO_3)_2$ (Baker, Analyzed), $CdCl_2$ (Baker, Analyzed) and $TlNO_3$ (K & K Laboratories), respectively. All solutions were prepared with doubly distilled water.

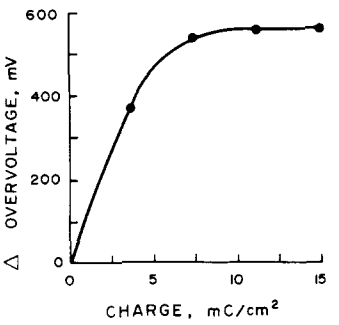

Figure 1. Change in hydrogen overvoltage with amount of mercury deposited on nickel minigrid. Charge in mC/cm² of microscopic area (1 mC = 5.18 × 10^{-6} mmol of mercury). 0.6m*M* Hg^{2+}, 0.1*N* HCl, 0.5*M* KCl

Procedure. The following procedure gave a mercury–nickel electrode with greatest hydrogen overvoltage and longevity. A nickel minigrid optically transparent thin layer electrode was subjected to fifteen minutes of radiofrequency discharge cleaning (Plasma Cleaner, Harrick Scientific Company, Ossining, NY) immediately before the mercury-deposition procedure to remove any organic film on the grid and the inner surface of the glass. This step was very useful for minimizing air bubble entrapment in the cell. Electrodes were then prepared by drawing a solution of ca. 0.5m*M* Hg^{2+}, 0.1*M* HCl, 0.5*M* KCl into the cell. A potential of −1.10 V vs. SCE was then applied to the nickel grid and maintained until hydrogen evolution was apparent from bubble formation. This deposition was repeated on fresh solution aspirated into the thin layer cell for a total of nine depositions. The cell was then rinsed thoroughly with doubly distilled water. The nine depositions correspond to ca. 1.6 × 10^{-4} mmol of mercury deposited on the total nickel minigrid. This is 1.5 × 10^{-4} mmol/cm² or 29 mC/cm² on the *microscopic* surface area of the grid. [A 1.0-cm × 1.8-cm piece of minigrid has a microscopic surface area, the calculated surface area of the bars of the grid (*14*), of 1.1 cm².] This amount of mercury corresponds to a film thickness of ca. 200 Å, assuming a uniform deposit.

Hydrogen evolution begins at the bottom of the transparent electrode and the bubbling action quickly advances to the top of the electrode. This is a consequence of the ohmic potential drop in the solution. It is considered that the ohmic potential drop is low enough so that uniform deposition of mercury occurs over the electrode surface. This fact is substantiated by observation of the rapid (2–3 sec) color change from dark gray to a flat, light gray hue of the electrode during mercury deposition.

Equally good electrodes could be prepared from more depositions with less concentrated Hg^{2+} solutions. However, electrodes prepared with more concentrated solutions of Hg^{2+}, and fewer depositions exhibited noticeably poorer hydrogen overvoltage and longevity characteristics even though equivalent amounts of mercury were deposited.

Some electrodes were prepared by deposition from mercuric solutions of higher pH. Successively more negative deposition potentials were applied as the pH increased to ensure sufficient hydrogen evolution (−1.2 V for pH 4.0, −1.6 V for pH 7.0).

Removal of dissolved oxygen from the thin layer cell was accomplished by applying a potential of −0.83 V vs. SCE for three minutes, causing reduction of O_2 to H_2O at the working electrode.

No particular precautions were taken in storing the electrodes between experiments. All electrodes were left exposed to air.

RESULTS AND DISCUSSION

Hydrogen Overvoltage and Scanning Electron Microscopy. Since an important property of mercury as an electrode material is its substantial hydrogen overvoltage, the shift in hydrogen overvoltage from its value on pure nickel was evaluated as a function of the amount of mercury deposited on the nickel minigrid. The increase in hydrogen overvoltage as a function of the amount of mercury deposited in millicoulombs per cm² piece of minigrid is shown in Figure 1. (Hydrogen overvoltage was measured as the

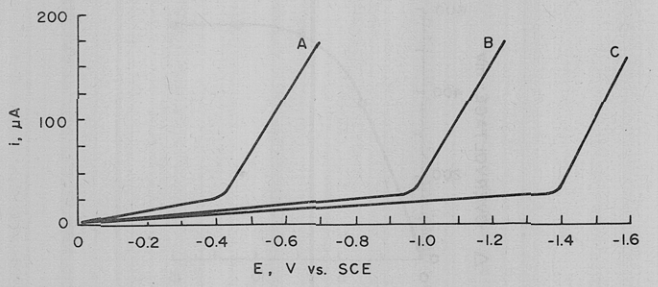

Figure 2. Comparison of three electrodes by current–voltage curves. Scan rate, 5 mV sec^{-1}; 0.5*M* KCl, 0.1*N* HCl

(*A*) Ni optically transparent thin layer electrode. (*B*) Hg–Ni optically transparent thin layer electrode. (*C*) Hanging mercury drop electrode

potential at which the current reached 25 μA.) The hydrogen overvoltage was shifted 500–600 mV by deposition of ca. 10 mC/cm^2 of mercury. No additional increase was obtained by depositing larger amounts of mercury. Controlling the applied potential during deposition so that hydrogen evolution occurred concurrently with mercury deposition was important in achieving the maximum hydrogen overvoltage. Failure to evolve hydrogen resulted in poorer hydrogen overvoltage of the resulting electrode by about 100 mV.

Electrodes prepared by deposition from mercuric solutions of higher pH (4.0 and 7.0) gave curves which were similar in shape to that in Figure 1. However, the electrodes which were prepared at pH 1.0 gave the best hydrogen overvoltages when subsequently used in solutions ranging in pH from 1.0 to 10.0.

The Hg–Ni electrode prepared by deposition of mercury at pH 1.0 functioned well in solutions of varying pH. A plot of the hydrogen overvoltage as a function of pH for a typical Hg–Ni electrode was linear with a slope of −60.6 mV/pH. The potentials at which hydrogen evolution occurred as a function of pH are as follows: pH 1.0, $E = -0.73$ V; pH 4.0, $E = -0.91$ V; pH 7.0, $E = -1.09$ V; pH 10.0, $E = -1.28$ V.

The hydrogen overvoltage of the mercury film electrode was intermediate between that of a pure nickel minigrid and that obtained on a pure mercury drop. This is illustrated in Figure 2 by current–potential curves obtained on the three electrodes at pH 1.0. The increase in hydrogen overvoltage of 600 mV falls short of the overvoltage on pure mercury by about 400 mV. Similar behavior was observed with solutions of pH 4.0, 7.0, and 10.0.

The inability to achieve the hydrogen overvoltage of pure mercury on the mercury-coated nickel minigrids is attributed to the thinness of the mercury film. Figure 3 shows scanning electron microscope photographs of the nickel minigrid with and without the deposited mercury film. The physical nature of the mercury deposit is primarily a uniform film, which smooths the surface roughness of the nickel, with occasional mercury droplets. Since a mercury deposit of 29 mC/cm^2 corresponds to an average mercury layer thickness of only 200 Å it is reasonable that contamination of the mercury film by amalgamation with the substrate nickel may occur shortly after deposition. The catalytic effect of this dissolved nickel would diminish the hydrogen overvoltage of the mercury. Nickel and mercury form various intermetallic compounds such as $Ni(Hg)_2$, $Ni(Hg)_3$, and $Ni(Hg)_4$ which would also be expected to contribute to diminished hydrogen overvoltage (*15*). Similar arguments have been advanced for thin mercury films on platinum substrates (*13, 16*).

The increase in hydrogen overvoltage for mercury on

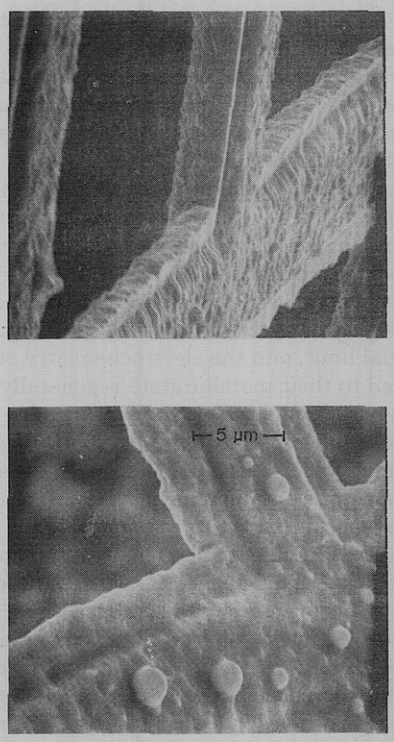

Figure 3. Scanning electron micrographs.

(*A*) Nickel minigrid (top). (*B*) Mercury-coated nickel minigrid (bottom)

nickel is greater than that obtained for comparable thicknesses of mercury on platinum optically transparent electrodes (*13*). This is possibly a result of being able to evolve hydrogen simultaneously with deposition of Hg on the nickel grid. Although this procedure is not feasible on the thin platinum films, evolution of hydrogen has been shown to have a beneficial effect on the hydrogen overvoltage of thicker mercury films deposited on bulk platinum (*17*). A contributing factor could also be the fact that nickel is less soluble in mercury than platinum is, thus diminishing the amount of substrate metal at the electrode surface in the Hg–Ni electrode as compared to the Hg–Pt electrode (*18*).

The effects of slow amalgamation were evident in the time-dependent behavior of the electrode. The maximum hydrogen overvoltage existed immediately after mercury deposition and gradually diminished during subsequent use. A typical hydrogen overvoltage decrease was 100 mV in eight hours of use after deposition. This was presumably the result of gradual contamination of the mercury film by nickel amalgamation.

The initial, maximum hydrogen overvoltage could be renewed for a used electrode by depositing an additional 10–15 mC/cm^2 of Hg. Such "regeneration" of the optimum hydrogen overvoltage was commonly done at the beginning of each day during the course of this experimental work. A single electrode treated in this manner could typically be used for about three weeks with an additional "regenerating" deposit each day. More frequent regenerations were necessary when working near the hydrogen overvoltage limit where small decreases in overvoltage interfered with the reduction process of interest. Electrodes which were not used for months after the initial mercury deposit could also be regenerated. The limiting factor for useful lifetime of a particular grid was the eventual accumulation of sufficient mercury to dissolve the substrate nickel. Therefore, longevity could be increased by depositing the minimum amount of mercury requisite for maximum hydrogen overvoltage. Hydrogen overvoltage of a used electrode could

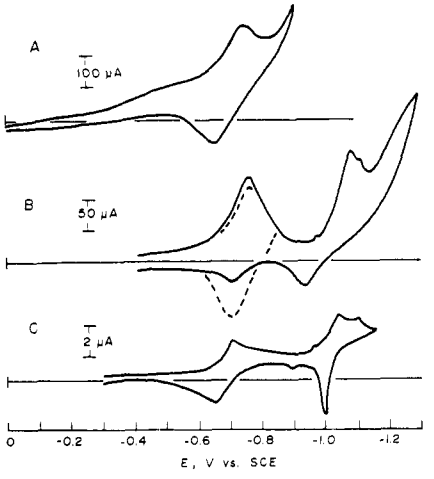

Figure 4. Cyclic voltammograms of 1.0m*M* MV^{2+}, 0.1*M* phosphate buffer pH 7.0, 0.1*M* NaCl. Deoxygenated for 30 minutes with pure nitrogen.

(*A*) Au thin layer cell, scan rate 2 mV sec^{-1}. (*B*) Hg–Ni thin layer cell, scan rate 5 mV sec^{-1}. (*C*) Hanging mercury drop electrode, scan rate 20 mV sec^{-1}

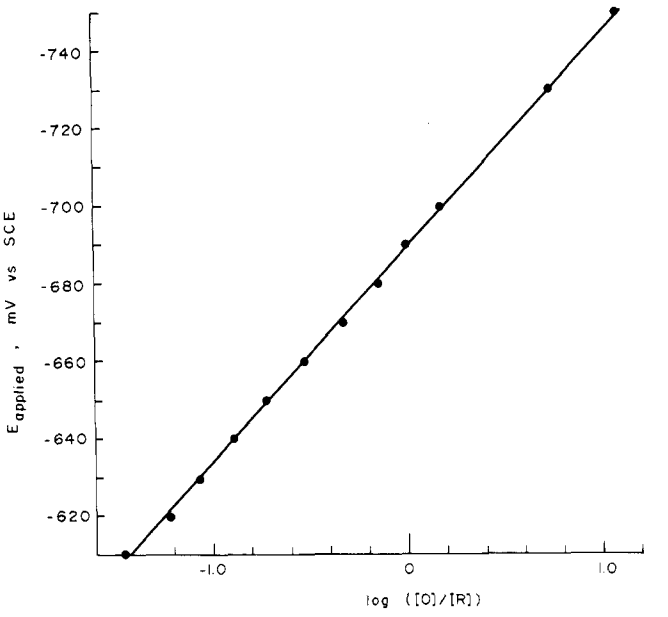

Figure 5. Plot of $E_{applied}$ vs. log($[MV^{2+}]/[MV^{\cdot+}]$) for 1.0m*M* MV^{2+}, 0.1*M* NaCl, 0.1*M* phosphate buffer pH 7.0

also be improved about 50 mV by simply evolving hydrogen for a few minutes.

Anodic Properties. The anodic limit of a typical Hg–Ni electrode was about +0.5 V in pH 7.0, 1.0*M* Na_2SO_4 solution (*19*). The mercury deposit could be removed by electrochemical oxidation only immediately after the first deposition. Oxidative removal after successive depositions of mercury caused the electrode to turn black, and ultimately resulted in physical dissolution of the minigrid. Apparently, this was caused by simultaneous oxidation of the nickel substrate.

Demonstration of Optical Applicability. Deposition of the small amounts of mercury reported here caused no measurable attenuation in optical transparency of the minigrid. This is due to the large hole size relative to the dimensions of the nickel framework. Consequently, the transmittance of the Hg–Ni electrode was essentially that reported by the manufacturer for the Ni minigrid, 57% for the 333 lpi grid used here.

The utility of the improved hydrogen overvoltage of the Hg–Ni electrode was demonstrated by measurements on methyl viologen dication (MV^{2+}). Potential scan experiments have shown that MV^{2+} undergoes two consecutive one-electron reduction waves to form $MV^{\cdot+}$ and MV^0 (20).

$$MV^{2+} + e^- \rightleftarrows MV^{\cdot+}$$
$$MV^{\cdot+} + e^- \rightleftarrows MV^0$$

Figure 4*A* shows a cyclic voltammogram for MV^{2+} in pH 7.0 buffer with a gold minigrid thin layer cell. The hydrogen evolution wave distorts the first reduction wave to $MV^{\cdot+}$ and completely obscures the second reduction wave to MV^0. A cyclic voltammogram of the same solution with the mercury film thin layer cell is shown in Figure 4*B*. In this case, both one-electron waves are easily distinguishable from the onset of hydrogen evolution. The small reduction "bumps" at −0.95 and −1.10 V are believed to be effects of MV^0 adsorption on the electrode. The oxidation peaks were diminished when the potential was scanned into hydrogen evolution as shown by the solid line. The dotted line shows a cyclic voltammogram of the first reduction wave only with a normal oxidation peak. A cyclic voltammogram which was obtained on a hanging mercury drop electrode is shown in Figure 4*C*. The sharp oxidation wave for MV^0 to $MV^{\cdot+}$ is the characteristic shape for oxidation of an adsorbed species. This sharp peak was diminished on the second and subsequent scans so that the voltammogram's appearance became similar to that shown for the mercury film electrode by the solid line in Figure 4*B*.

With the mercury minigrid electrode, it was possible to obtain a value for $E^{0'}_{MV^{2+},MV^{\cdot+}}$ by the recently reported spectropotentiostatic technique where the ratio $[MV^{2+}]/[MV^{\cdot+}]$ in the thin layer cell was controlled by an applied potential (*12*). This measurement was not possible in the previous study because of the hydrogen evolution interference on the gold minigrid. Figure 5 shows a Nernstian plot of $E_{applied}$ vs. log ($[MV^{2+}]/[MV^{\cdot+}]$) where $[MV^{2+}]/[MV^{\cdot+}]$ for each applied potential was determined optically by monitoring $[MV^{\cdot+}]$ with 605 nm light passing through the thin layer cell. The potential intercept is −688 mV (std dev = 1.6 mV, N = 4) vs. SCE which corresponds to an $E^{0'}$ value of −446 mV vs. NHE. This agrees with reported values of −446 ± 5 mV (*21*) and −449 ± 2 mV (*20*). An n value of 1.06 was determined from the slope of 55.8 mV.

The extended cathodic range has also proven valuable in spectroelectrochemical thin layer studies of vitamin B_{12} (*19, 22*).

Metal Deposition. The Hg–Ni minigrid exhibited substantial mercury character for reduction of metal ions to the metallic form and for their subsequent oxidation.

A cyclic voltammogram for a solution of Pb^{2+} and Cd^{2+} is shown in Figure 6. The first reduction ($E_{p(c)}$ = −0.55 V) is lead, the second ($E_{p(c)}$ = −0.83 V) is cadmium. The sharpness of these reduction waves is characteristic of thin layer voltammetry where complete electrolysis in the thin layer is rapid as a result of the short diffusional path (0.02 cm in this case). The anodic "stripping" peaks corresponding to oxidation of the metal which had amalgamated into the thin mercury film during reduction are also sharp. Here the diffusional path is the thickness of the mercury film which was only 200 Å on this electrode. The sharpness of these stripping peaks suggested possible utility of the Hg–Ni thin layer cell for analysis.

For solution concentrations below about $10^{-3}M$, single stripping peaks were obtained for a given metal as is characteristic of mercury electrodes. Multiple peaks, which typ-

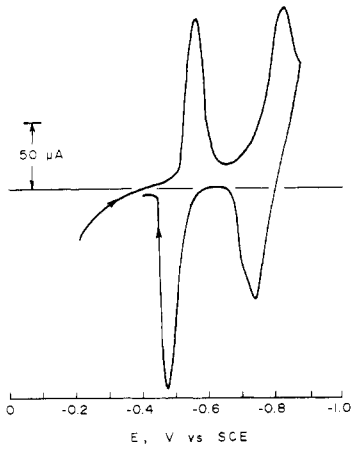

Figure 6. Cyclic voltammogram of 1m*M* Pb^{2+}, 0.5m*M* Cd^{2+} mixture in 0.1*N* HCl, 0.5*M* KCl. Hg–Ni thin layer cell. Scan rate, 2 mV sec^{-1}

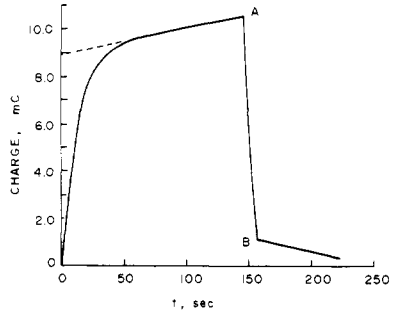

Figure 7. Charge–time curve for application of potential step from −0.350 V to −0.600 V to −0.350 V vs. SCE. Hg–Ni thin layer cell. 1.12m*M* Pb^{2+}, 0.1*M* KNO_3, 0.1*N* HNO_3

ify the behavior of metal deposition on solid electrodes, were not observed.

Anodic Stripping Coulometry. An important characteristic of thin layer cells is the short time required for complete electrolysis in the thin layer during controlled potential coulometry (*23, 24*). Figure 7 shows a typical charge–time curve (chronocoulogram) for 1.12m*M* Pb^{2+} in a Hg–Ni thin layer cell. The Pb^{2+} in the thin layer was first deposited in the Hg film by reduction at −0.600 V and then stripped out by oxidation at −0.350 V. Examination of the resulting charge–time behavior shows that complete reduction was achieved in about 40 seconds whereas complete oxidation required only 5 seconds. This reflects the different thicknesses of the aqueous and mercury phases as mentioned above.

The amount of Pb^{2+} in a sample solution could be determined from the charge for either complete reduction or oxidation by Faraday's Law

$$Q = nFVC \quad (1)$$

where V is the volume of the thin layer of solution surrounding the working electrode. The charge for reduction was measured by extrapolating the Q–t curve to 0 seconds; the oxidation charge was taken as the difference between point A and the inflection point B. In both cases corrections for background charge were applied (*23*). Comparison of Q reduction with Q oxidation showed complete recovery of electroactive species. The lead could be quantitatively cycled between Pb^{2+} in solution and Pb^0 in the mercury film. More precise values of Q were obtainable from the stripping charge than from the reduction charge because of

Table I. Analysis of Pb^{2+} by Anodic Stripping Coulometry[a]

$[Pb^{2+}]$ μg/ml			
Known	Measured	Std dev	N
53.6	46.2	1.99	3
	49.3		
	49.9		
	$\bar{x}$ = 48.5		
213	211	3.46	3
	211		
	209		
	$\bar{x}$ = 210		
267	253	3.16	3
	255		
	261		
	$\bar{x}$ = 256		

[a] Cell volume 3.16 × 10^{-5} l. Calibrated with 160 μg/ml Pb^{2+}.

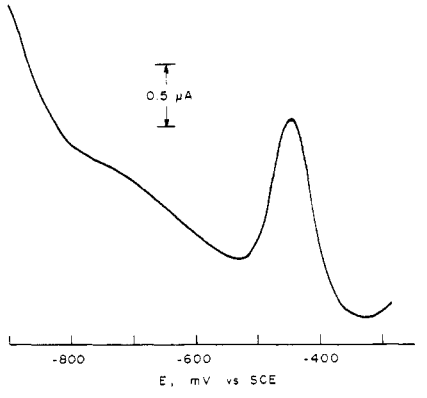

Figure 8. Differential pulse anodic stripping voltammogram of 36 ng/ml Pb^{2+}, 0.1*M* HNO_3, 0.1*M* KNO_3 in a Hg–Ni thin layer cell. ν = 0.5 mV/sec; 10-mV pulse every 2 sec; initial potential −900 mV vs. SCE

the sharp inflection at complete oxidation (point B). Consequently, a procedure was used whereby, for each analysis, lead was deposited in the mercury film and dissolved oxygen reduced to water by applying a potential of −0.900 V for 5 minutes. The potential was then stepped to −0.350 V and the Q–t curve for lead stripping was recorded. Table I shows typical results which were obtained for analysis of known lead solutions by this procedure for anodic stripping coulometry. The detection limit of the method is about 10 μg/ml.

Differential Pulse Anodic Stripping Voltammetry. One of the most sensitive electroanalytical techniques is differential pulse anodic stripping voltammetry (*25, 26*). Combining this technique with the thin layer cell greatly improved the analytical sensitivity as compared to anodic stripping coulometry. Figure 8 shows a differential pulse anodic stripping voltammogram of 36 ng/ml Pb^{2+} in a mercury film thin layer cell. In this case, the metal ions in the thin solution layer were deposited into the mercury film of the thin layer cell by the same procedure described above for anodic stripping coulometry. The electrodeposited metals were then anodically stripped from the mercury film by differential pulse anodic stripping voltammetry. Very sharp stripping peaks were obtained.

Perhaps the most significant characteristic of the thin layer cell from the analytical point of view is its small vol-

ume capability (less than 50 μl). Coupling the sensitivity of differential pulse anodic stripping voltammetry with the small volume of the thin layer cell results in a method which is potentially useful for trace analysis on very small amounts of sample material. It should also be noted that the complete electrolysis aspect of the thin layer cell during the deposition step eliminates some of the uncertainties attendant in the deposition step with conventional differential pulse anodic stripping voltammetry at a hanging mercury drop electrode, i.e., variations in drop size, stirring conditions, and deposition time.

CONCLUSION

An optically transparent thin layer electrochemical cell with substantial mercury character has been demonstrated. The electrode is easily made with available materials and is easy to use. The good optical transparency and hydrogen overvoltage make it useful for spectroelectrochemical studies in the negative potential region. The electrode has potential utility for the analysis of metal ions by anodic stripping coulometry and differential pulse anodic stripping voltammetry, particularly when the small volume capability of the thin layer cell is necessary.

ACKNOWLEDGMENT

The authors gratefully acknowledge B. J. Norris for the cyclic voltammogram of MV^{2+} on the gold minigrid and J. P. Haberman and D. A. Hudson, The Procter and Gamble Company, Cincinnati, OH, for the scanning electron microscope photographs.

LITERATURE CITED

(1) T. Kuwana, *Ber. Bunsenges. Phys. Chem.*, **77**, 858 (1973).
(2) N. Winograd and T. Kuwana in "Electroanalytical Chemistry", Vol. 7, A. J. Bard, Ed., Marcel Dekker, New York, NY, 1974.
(3) "Advances in Electrochemistry and Electrochemical Engineering", Vol. 9, R. H. Muller, Ed., John Wiley, New York, NY, 1973.
(4) R. W. Murray, W. R. Heineman, and G. W. O'Dom, *Anal. Chem.*, **39**, 1666 (1967).
(5) A. Yildiz, P. T. Kissinger, and C. N. Reilley, *Anal. Chem.*, **40**, 1018 (1968).
(6) W. R. Heineman, J. N. Burnett, and R. W. Murray, *Anal. Chem.*, **40**, 1970 (1968).
(7) W. R. Heineman, J. N. Burnett, and R. W. Murray, *Anal. Chem.*, **40**, 1974 (1968).
(8) T. E. Neal and R. W. Murray, *Anal. Chem.*, **42**, 1654 (1970).
(9) I. Piljac and R. W. Murray, *J. Electrochem. Soc.*, **118**, 1758 (1971).
(10) G. Peychal-Heiling and G. S. Wilson, *Anal. Chem.*, **43**, 550 (1971).
(11) V. S. Srinivasan and F. C. Anson, *J. Electrochem. Soc.*, **120**, 1359 (1973).
(12) W. R. Heineman, B. J. Norris, and J. F. Goelz, *Anal. Chem.*, **47**, 79 (1975).
(13) W. R. Heineman and T. Kuwana, *Anal. Chem.*, **44**, 1972 (1972).
(14) M. Petek, T. E. Neal, and R. W. Murray, *Anal. Chem.*, **43**, 1069 (1971).
(15) A. Baranski and Z. Galus, *Electroanal. Chem. Interfac. Electrochem.*, **46**, 289 (1973).
(16) W. R. Heineman and T. Kuwana, *Anal. Chem.*, **43**, 1075 (1971).
(17) A. M. Hartley, A. G. Hiebert, and J. A. Cox, *J. Electroanal. Chem.*, **17**, 81 (1968).
(18) "Comprehensive Inorganic Chemistry", Vol. 3, Pergamon Press Ltd., Oxford 1973, pp 283–285.
(19) T. M. Kenyhercz, T. P. DeAngelis, B. J. Norris, W. R. Heineman, and H. B. Mark, Jr., *J. Am. Chem. Soc.*, submitted for publication.
(20) E. Steckhan and T. Kuwana, *Ber. Bunsenges. Phys. Chem.*, **78**, 253 (1974).
(21) M. Ito and T. Kuwana, *J. Electroanal. Chem.*, **32**, 415 (1971).
(22) T. M. Kenyhercz, A. M. Yacynych, and H. B. Mark, Jr., *J. Am. Chem. Soc.*, submitted for publication.
(23) C. N. Reilley, *Rev. Pure Appl. Chem.*, **18**, 137 (1968).
(24) A. T. Hubbard and F. C. Anson in "Electroanalytical Chemistry", Vol. 4, A. J. Bard, Ed., Marcel Dekker, New York, NY, 1974.
(25) J. B. Flato, *Anal. Chem.*, **44** (11), 75A (1972).
(26) T. R. Copeland and R. K. Skogerboe, *Anal. Chem.*, **46**, 1257A (1974).

RECEIVED for review December 2, 1974. Accepted March 18, 1975. The authors gratefully acknowledge the financial support provided by National Science Foundation Grant GP-41981X.

Use of Optically Transparent Thin-Layer Cells for Determination of Composition and Stability Constants of Metal Ion Complexes with Electrode Reaction Products

Ivan Piljac,[1] Mihael Tkalčec, and Božidar Grabarić

Laboratory of Inorganic Chemistry, Faculty of Technology, University of Zagreb, POB 179, 41001 Zagreb, Croatia, Yugoslavia

It was demonstrated that the optically transparent thin-layer (OTTL) cells are a very convenient tool for investigation of interactions between metal ions and electrode reaction products. For this purpose, a simple small volume OTTL cell allowing better control of gold minigrid working electrode potential was constructed. The composition and stability constants of Li^+ complexes with one- and two-electron product of 1-hydroxy-9,10-anthraquinone (HOAQ) and one-electron product of 9,10-anthraquinone (AQ) was determined.

Since 1964 when Kuwana, Darlington, and Leedy (*1*) introduced the tin-oxide coated glass as a transparent working electrode for monitoring the course of an electrochemical reaction, the optically transparent electrodes and cells have found a variety of applications (*2*). A gold minigrid electrode for spectroelectrochemical thin-layer cells was introduced by Murray, Heineman, and O'Dom (*3*). In the previous paper (*4*), an elaboration of such an OTTL cell with gold minigrid was employed in measurements of coulometric electrolysis charges and product spectra of HOAQ in several aprotic solvents. It has been found that HOAQ is reduced in two one-electron steps to a stable radical anion ($HOAQ\cdot^-$) and a dianion ($HOAQ^{2-}$) on an OTTL electrolysis time scale in *N,N*-dimethylformamide (DMF) solutions.

In the present work an improved model of the OTTL cell has been used in determination of composition and stability constants of Li^+ complexes, and a visible absorption

[1] Author to whom correspondence should be addressed.